

# Autonomous COLREGs-Compliant Decision Making using Maritime Radar Tracking and Model Predictive Control\*

D. K. M. Kufoalor, E. Wilthil, I. B. Hagen, E. F. Brekke, T. A. Johansen

**Abstract**—This paper addresses the challenges of making safe and predictable collision avoidance decisions considering uncertainties related to maritime radar tracking. When a maritime radar is used for autonomous collision avoidance, strategies for handling uncertain obstacle tracks, false tracks, and track loss become necessary. Robust decisions are needed in order to achieve clear and predictable actions according to the international regulations for preventing collisions at sea (COLREGs). We present robustness considerations and results of using an Integrated Probabilistic Data Association (IPDA) tracking method with a collision avoidance method based on Model Predictive Control. The results are from full-scale experiments that cover challenging multiple dynamic obstacle scenarios, including realistic vessel interactions where some obstacles obey COLREGs, while others do not.

## I. INTRODUCTION

Maritime collision avoidance is a challenging task that has been studied for many years, and the technology for safe navigation of marine vessels have evolved over the years. However, most of the existing technology is mainly intended as an aid to the human operator. The human operator makes a decision by evaluating the collision risk, using the information available about obstacles obtained from different sources, e.g. lookout, radar and nautical chart plotters, Automatic Identification System (AIS), and Vessel Traffic Service (VTS). Due to the reliance on a human operator, the reliability and accuracy of the existing automatic obstacle detection/tracking systems may not be the most crucial factors in the decision making process.

The existing “rules of the road” were also developed for the human operator, and therefore do not generally provide quantitative criteria for both the assessment of a potential collision situation and the actions needed to avoid collisions. Furthermore, COLREGs advocate “good seamanship” (see e.g. Rules 2 and 8 of [1]), probably due to the uniqueness of every situation and the characteristics of the maritime domain that make the collision avoidance task challenging. Specifically, the decision process needs to consider, among other factors, a large variety of obstacles, different sea states, dynamic motion in 2D space, and uncertainty in both sensor information and (intended) motion of obstacles in different environmental conditions. In view of the above observations,

All authors are with the Center for Autonomous Marine Operations and Systems (AMOS), Department of Engineering Cybernetics, Norwegian University of Science and Technology (NTNU), O.S. Bragstads plass 2D N-7491 Trondheim, Norway. {kwame.kufoalor, erik.wilthil, inger.b.hagen, edmund.brekke, tor.arne.johansen}@ntnu.no

\* This work was supported by the Research Council of Norway (NFR) through the projects 223254 and 244116/O70. The professorship of Edmund Brekke is funded by DNV GL

we acknowledge the difficulty of making the decision process autonomous, especially, based on existing technology and rules. An autonomous surface vehicle (ASV) must be able to rely on its sensors and should implement a decision strategy that is robust to uncertain information available for collision avoidance.

The maritime radar, which is a primary sensor for safe maritime navigation is useful in combination with effective obstacle tracking algorithms for autonomous collision avoidance if it produces accurate estimates of obstacle tracks, and has a low rate of false tracks and track loss. Different implementations and experimental validation of maritime target tracking algorithms are provided in [2], [3], [4]. A crucial aspect is to find a useful balance between false alarm rate and track initiation time in order to avoid detecting targets too late and also to reduce the risk of making wrong collision avoidance actions [2].

Earlier work that discuss the challenges of using maritime radar for autonomous collision avoidance include [5], [6]. While both focus on close-range situations, [5] assumes no track loss occurs, and the reactive method in [6] does not implement COLREGs compliance. Different methods that aim at COLREGs compliance are treated in [7], [8], [9], [10], [11], and some reviews of existing maritime collision avoidance methods can be found in [12], [13]. As noted in [8], different limitations in some of the existing collision avoidance methods motivate the use of ideas from optimization based control, which typically lead to a straightforward approach to specifying constraints and objectives.

In this paper, we explore the potentials of using the estimated maritime radar tracks from an Integrated Probabilistic Data Association (IPDA) tracking method in a Scenario-based Model Predictive Control (SB-MPC) decision framework. The main contributions include robustness considerations in the IPDA method, and the treatment of different uncertainties associated with maritime radar tracking in SB-MPC without using uncertainty estimates from the tracking method. The work in [8] and [14] is extended by introducing uncertainty adapted predictions of obstacle motion and a strategy for reducing the adverse effect of false/lost tracks. The overall collision avoidance system is suitable for both long-range and close-range encounters. Our approach leads to collision avoidance decisions that comply with COLREGs, by prioritizing deliberate early, clear, predictable actions. We also present full-scale experiments covering different dynamic multi-obstacle scenarios, using an ASV that implements the architectural components shown in Fig. 1.

The remainder of this paper is structured as follows:

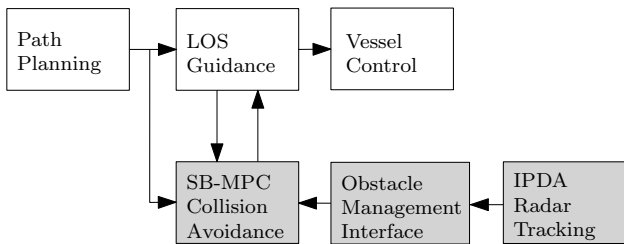


Fig. 1: ASV functional interface setup. The white boxes are existing functions, and the gray boxes are tracking, obstacle management, and collision avoidance functions presented in this paper.

Sections II–III describe the radar tracking method, the collision avoidance method, the uncertainties, and the related robustness considerations made in this work. Presentation and discussion of the experimental results follow in Section IV, and concluding remarks are given in Section V.

## II. MARITIME RADAR TRACKING

### A. Radar tracking method

The backbone of the radar tracking system is described in [2], which implements a single-target tracking method. Through a parallel implementation of filters the tracking method is capable of tracking multiple targets when the targets are sufficiently separated in the state space. The tracking system uses one target motion model, a nearly constant velocity (NCV) model [15], which assumes that the target moves according to the linear Gaussian model

$$p(x_{j+1}|x_j) = \mathcal{N}(F_j x_j, Q_j), \quad (1)$$

where  $\mathcal{N}$  is the probability density function of the normal distribution,  $x_j = (p_N, v_N, p_E, v_E)$  is the state of the target at time  $j$ , consisting of, respectively, the North and East positions and velocities in a stationary North East Down (NED) reference frame. The state transition matrix  $F_j$  and the process noise covariance matrix  $Q_j$  in (1) are defined as follows:

$$F_j = \begin{bmatrix} F_1 & 0_{22} \\ 0_{22} & F_1 \end{bmatrix}, \quad F_1 = \begin{bmatrix} 1 & T_r \\ 0 & 1 \end{bmatrix},$$

$$Q_j = \begin{bmatrix} Q_1 & 0_{22} \\ 0_{22} & Q_1 \end{bmatrix}, \quad Q_1 = q \begin{bmatrix} T_r^4/4 & T_r^3/2 \\ T_r^3/2 & T_r^2 \end{bmatrix}.$$

$T_r$  is the sampling time (i.e. the time between two radar scans),  $q$  is the process noise covariance parameter, and  $0_{22}$  is a  $2 \times 2$  zero matrix. The observation model used is

$$p(z_j|x_j) = \mathcal{N}(Hx_j, R_j), \quad (2)$$

where the matrix  $H$  extracts  $z_j = (p_N, p_E)$  from  $x_j$ , and  $R_j$  is the measurement noise covariance matrix. The above model captures the typical straight-line motion of marine vessels.

The Integrated Probabilistic Data Association (IPDA) method presented in [16] is used for track initiation and track maintenance. The fundamental principle of the IPDA [17] is to calculate an existence probability for each track, based on the innovations of the measurements in the vicinity

of the track, i.e. the difference between the measurements and their expected value based on the prior state estimate. Initially, tracks are categorized as preliminary tracks, which is only used internally in the tracking system. When the existence probability exceeds a given threshold  $P_C$ , the track is confirmed as a valid target. Tracks are terminated if the existence probability falls below another threshold  $P_T$ .

The output of the radar tracking system consists of a list of confirmed targets, each with an ID and estimates of the target's position  $(p_N, p_E)$ , speed  $u$ , and course  $\chi$ . The speed and course are, respectively, the magnitude and direction (angle) of the velocity vector  $(v_N, v_E)$ . The estimates from the tracking system are considered as obstacle measurements used in the COLREGs-compliant decision method described in Section III. Every new track is given a new ID, which means that after a track is terminated, a new track that appears on the same target gets a new ID.

In this paper, we focus on the consequences of the assumptions made in the tracking system and the related uncertainties that a collision avoidance method needs to consider in its decision process. By not using uncertainty estimates computed by the tracking method in the COLREGs-compliant decision method, we obtain a collision avoidance system that does not depend on uncertainty representations specific to the implemented tracking method. We also avoid COLREGs-compliant method-specific representations in the tracking method that may lead to a more complicated (tightly-coupled) tuning procedure. For instance, prolonging the life of tracks in the tracking system based on their impact on collision avoidance decisions requires conservative tuning that produces many false tracks. Further details of the tracking system can be found in [2] and [16].

### B. Radar track uncertainty

Radar tracking of obstacles introduces both data association uncertainty and state estimation uncertainty, i.e. position and velocity estimation errors, into a collision avoidance decision process.

The accuracy of data association in the tracking method is evident in the absence/presence of false tracks and the rate of track loss. In the IPDA tracking method used, premature track termination can be delayed by choosing a high value for the survival probability of the IPDA. This means that the existence probability will not be reduced below the threshold until several misdetections have occurred. This also increases the expected lifetime of any false track that appears. In practice, a useful balance is determined through tuning, and the collision avoidance decisions must be robust to both false tracks and track loss.

Due to the NCV model used in the tracking method, track loss may occur when the target is maneuvering. By choosing the process noise parameter  $q$  of the motion model process noise covariance properly, most of the typical maneuvers are captured by the NCV model. Additionally, the fast track initiation/establishment capabilities of the IPDA (see [16]) implies that the duration of track loss may not be significant in this case, since new tracks may appear, and may be used to

trace the maneuvering path of the target. If the maneuvers are not sufficiently followed by the NCV model, an interacting multiple model (IMM) approach can be used [18]. Note that using an IMM does not necessarily avoid this issue entirely since one needs to deal with a more complex procedure that switches between models, and handling of cases where different models attain similar likelihoods (in a probabilistic framework) may not be a trivial task (see e.g. [5]).

The tracking system also influences the collision avoidance through fluctuations in the state estimate. In particular, the speed and course estimation errors can have a large impact on long-range collision prediction, as a small change of course may lead to a large change of position at the end of the prediction interval. This is remedied by representing the range-dependent measurement noise in the tracking system on a polar form, which is transformed into a Cartesian frame [18], instead of working directly with the uncertainty in the Cartesian frame as done in [2]. This provides less fluctuating estimates of the target course and speed when it is tracked from a long range.

### III. COLREGS-COMPLIANT DECISION

In this section, we briefly describe our COLREGS-compliant decision method, and we propose different implementation strategies that enhance robustness to the radar tracking uncertainties discussed in Section II-B.

#### A. COLREGS-compliant decision method

The scenario-based MPC (SB-MPC) COLREGS-compliant decision method in [8] and the implementation of [14] is used in this work, with some extensions. The method solves the following optimization problem

$$k^*(t_0) = \arg \min_k \mathcal{H}^k(t_0), \quad (3)$$

where

$$\begin{aligned} \mathcal{H}^k(t_0) = \max_i \max_{t \in \mathcal{D}(t_0)} & (l_i(t_{\text{lost}}) \cdot c_i(u_m^k, \chi_m^k, t) \\ & + \mu_i(u_m^k, \chi_m^k, t) + \tau_i(u_m^k, \chi_m^k, t)) \\ & + f(u_m^k, \chi_m^k) + g(u_m^k, \chi_m^k), \end{aligned}$$

using the set  $\mathcal{D}(t_0) = \{t_0, t_0 + T_s, \dots, t_0 + T\}$ , where  $T_s$  is the sampling time and  $T$  is the prediction horizon. We provide a brief description of the cost function components  $l_i, c_i, \mu_i, \tau_i, f, g$  in this section, and we refer to [8] and [14] for their detailed specifications.

The cost function  $\mathcal{H}^k(t_0)$  expresses the hazard associated with selecting a control behavior with index  $k$  and defined by course ( $\chi_m^k$ ) and speed ( $u_m^k$ ) modifications that are applied to corresponding desired reference values,  $\chi_d, u_d$ , for the course ( $\chi$ ) and speed ( $u$ ), respectively. We use the following set of alternative control behaviors, which we assume to be fixed on the prediction horizon:

- course offset in degrees:  $\chi_m^k \in \{-90, -75, -60, -45, -30, -15, 0, 15, 30, 45, 60, 75, 90\}$
- speed factor:  $u_m^k \in \{1, 0.5, 0\}$ , which translates to ‘keep speed’, ‘slow down’, or ‘stop’.

The function  $c_i$  denotes the cost of colliding with obstacle  $i$ , considering a collision risk that depends on the time and distance to the closest point of approach (CPA) and scales with the relative velocity of the obstacle and ASV. The allowed CPA is defined by a safety distance parameter  $d_{\text{safe}}$  and the obstacle’s length ( $L_i$ ). Specifically,  $d_{\text{safe}} + L_i/2$  is used to define the radius of a circular safety region, which encloses obstacle  $i$ .

We introduce the track-loss factor  $l_i(t_{\text{lost}})$ , which reduces the relevance of the collision cost of obstacle  $i$  when its track is terminated by the tracking system. The track-loss factor becomes smaller, the longer the track-loss duration ( $t_{\text{lost}}$ ) is, as specified in Section III-E. The cost of violating COLREGS is expressed by the function  $\mu_i$ , and  $\tau_i$  is a transitional cost that penalizes the termination of COLREGS-compliant maneuvers, in order to avoid unnecessary switching of control behaviors. The cost of maneuvering effort is specified by the function  $f$ , and  $g$  is a grounding cost that penalizes control behaviors that will result in collision with land or defined *no-go* zones.

The cost for each control behavior  $k$  at time  $t \in \mathcal{D}(t_0)$  is calculated based on the predicted state of the ASV and each obstacle  $i$ , obtained from the simulation of their trajectories. We simulate the trajectory of obstacle  $i$  using a kinematic model:

$$\dot{\eta}_i = R(\chi_i)v_i, \quad \eta_i = (x_i, y_i, \chi_i), \quad v_i = (v_{x_i}, v_{y_i}, r_i),$$

and a 3-degrees of freedom (DOF) model for the ASV:

$$\begin{aligned} \dot{\eta} &= R(\psi)v, \\ M\dot{v} + C(v)v + D(v)v &= \tau_u, \end{aligned}$$

where  $\eta = (x, y, \psi)$  denotes the position and heading in the earth-fixed frame,  $v = (v_x, v_y, r)$  represents the velocities in surge, sway, and yaw specified in the body-fixed frame. The matrices  $M, C(v), D(v)$  are the vessel inertia matrix, Coriolis, and damping, respectively.  $R(\psi)$  is a rotation matrix from body-fixed to earth-fixed frame, and  $\tau_u$  is the vector of control forces from an autopilot (a control law), which accepts the commanded reference,  $\chi_c = \chi_d + \chi_m^k$ ,  $u_c = u_d + u_m^k$ .

If estimates of environmental disturbances such as wind and current are available, it is recommended to include their effect in the 3-DOF model as shown in [8]. In our experiments, we use a feedback-linearization controller for speed control and a proportional-derivative controller for course control. Both controllers are included in the prediction model to provide the control forces  $\tau_u$ , which are used in the prediction of the ASV’s trajectory for each scenario  $k$ .

#### B. Inherent properties and robustness

An important property of the above hazard evaluation criterion is that it seeks the least conservative solution according to the given constraints, by prioritizing solutions that result in tangential maneuvers w.r.t. the boundary of the defined circular safety region. This implies that the collision avoidance decisions inherently lead to straight-line motion, which is considered as predictable behavior in a maritime environment.

Due to the implementation of a COLREGs-transitional cost  $\tau_i(\cdot)$ , it is straightforward to prioritize COLREGs-compliant maneuvers in long-range encounters. Moreover, using a collision cost  $c_i(\cdot)$  that scales with the collision time, range, and relative velocity, ensures that the SB-MPC strategy will choose an evasive maneuver if collision becomes imminent.

The main advantage of the SB-MPC strategy in terms of robustness to noise/uncertainty is the fact that the effect of all potentially uncertain variables that affect the collision avoidance decisions are evaluated in the cost function  $\mathcal{H}^k(t_0)$  over a long prediction horizon  $T$ . In combination with an adequate choice of sampling time  $T_s$  and a scenario grid of alternative control behaviors, the cost function provides a filtering effect that ensures that changes in each variable must be significant enough to produce a change in the decisions. Moreover, the collision cost  $c_i(\cdot)$  prioritizes avoiding collision hazards that are close in time over those that are more distant and usually more uncertain [8].

### C. ASV guidance uncertainty

We assume that the ASV state is accurately known and the ASV's motion controllers are capable of achieving the desired references for course and speed, by compensating for disturbances (i.e. environmental forces). This assumption leads to a simple SB-MPC implementation, which relies on the hazard  $\mathcal{H}^k(t_0)$  evaluation criterion in (3) in order to achieve safe decisions.

### D. Obstacle motion uncertainty

In the nominal case where the obstacle state is accurately known, using a constant velocity model for predicting obstacle motion is sufficient to avoid collision in many cases (see e.g. [8],[14]). However, some cases may be difficult to capture with a constant velocity model, and collision avoidance decisions may become highly reactive.

We propose a few extra scenarios that branch on the nominal scenario, by defining the following uncertainty-adapted sets that are used to predict the region occupied by the obstacle in the future:

$$\begin{aligned} \mathcal{U}_i &= \{\hat{u}_i - \bar{u}_{br1} - \tilde{u}, \hat{u}_i, \hat{u}_i + \bar{u}_{br2} + \tilde{u}\}, \\ \mathcal{\Psi}_i &= \{\hat{\chi}_i - \bar{\chi}_{br1} - \tilde{\chi}, \hat{\chi}_i, \hat{\chi}_i + \bar{\chi}_{br2} + \tilde{\chi}\}, \end{aligned}$$

where  $\tilde{u} = \min(\sigma_{u_i}, \bar{\sigma}_u)$  and  $\tilde{\chi} = \min(\sigma_{\chi_i}, \bar{\sigma}_\chi)$  are limits for specifying the extent of uncertainty adjustment allowed for the estimated speed  $\hat{u}_i$  and course  $\hat{\chi}_i$ , respectively. We consider obstacle speeds and course within one standard deviation ( $\sigma_{u_i}, \sigma_{\chi_i}$ ) around the mean, and we enforce the limits ( $\bar{\sigma}_u, \bar{\sigma}_\chi$ ) to ensure that initial estimates are within acceptable limits. The estimated speed, course, and their associated variances are obtained through an obstacle management interface (cf. Fig. 1) discussed in Section III-E.

The parameters  $\bar{u}_{br1}, \bar{u}_{br2}, \bar{\chi}_{br1}, \bar{\chi}_{br2}$  specify asymmetric branching offsets in speed and course, which account for a possible change in speed and course at the beginning of the prediction horizon. Therefore, the predicted region possibly occupied by the obstacle becomes larger further

into the prediction horizon. This does not pose feasibility issues in complex scenarios since the sets do not introduce hard constraints into the optimization problem (3). Moreover, branching the nominal (straight-line) predicted trajectory at the beginning of the horizon is still useful if the actual maneuver occurs later in the horizon since the predicted (conservative) region may still be valid. We choose asymmetric parameters, typically  $\bar{u}_{br1} = 1$  m/s,  $\bar{u}_{br2} = 0.1$  m/s,  $\bar{\chi}_{br1} = 1^\circ$ ,  $\bar{\chi}_{br2} = 5^\circ$ , because we expect obstacles that intend to follow COLREGs in dangerous situations to prefer starboard maneuvers over port, and may reduce speed, instead of increasing speed.

### E. Track loss and false tracks

We implement an obstacle management interface (see Fig. 1), which maintains a list of obstacles that have been previously used in the SB-MPC, and we manage this list separately from the obstacle list obtained from the tracking system. The intention is to be able to determine the impact of a track on the current collision avoidance decision based on its influence on previous decisions. The impact of a track depends on how long the track has been alive. This means that an obstacle that has been tracked for a while and suddenly terminated by the tracking system should not cause a (dangerous) abrupt change in behavior of the ASV.

Using a standard Kalman filter with relatively high measurement covariance values allows the SB-MPC algorithm to obtain position, speed, and course estimates that are close to the tracks received from the radar tracking system. The filter provides useful (open-loop) short-term predictions in case of track loss, without the need of keeping a long history of past states. If the track has been alive for less than a minimum tracking time  $t_{\min}^{\text{track}}$ , it is immediately discarded when terminated by the radar tracking system. Tracks that are used for at least  $t_{\min}^{\text{track}}$  are still considered in the hazard evaluation criterion  $\mathcal{H}^k(t_0)$  and the corresponding collision cost is reduced using the track-loss factor (cf. (3)):

$$l_i(t_{\text{lost}}) = \frac{T_s}{(t_{\text{lost}})^{q_l}}, \quad t_{\text{lost}} \geq T_s, \quad (4)$$

where  $t_{\text{lost}}$  is the track loss duration and  $q_l \geq 1$  is a tuning parameter. After a short duration  $\bar{t}_{\text{lost}}$ , or if the Kalman filter's error covariance estimates grow beyond a defined threshold, the track is discarded. This decision is based on the observation that real tracks that are (falsely) terminated will be regained quickly with a new ID (within  $\bar{t}_{\text{lost}}$ ), while false tracks or tracks that leave the radar sensing range may not return.

At close range to an obstacle, it is important that  $t_{\text{lost}}$  is kept as short as possible since a lost target may return with a new track that deviates significantly from the lost track (e.g. due to a sharp turn). However, the track-loss penalty ensures that the effect of a lost track diminishes quickly, giving priority to any new track that may pose a greater danger to the ASV. The above strategy also influences the effect of false tracks in the collision avoidance decisions.



(a) Telemetron (ASV) (b) Munkholmen II (c) Ocean Space Drone I

Fig. 2: Vessels involved in the experiments.

TABLE I: Vessel data: Ocean Space Drone I (OSD. I)

| Parameter       | ASV        | obstacles     |        |
|-----------------|------------|---------------|--------|
|                 | Telemetron | Munkholmen II | OSD. I |
| Length [m]      | 8.0        | 14.0          | 12.0   |
| Width [m]       | 3.0        | 6.0           | 3.0    |
| Max. speed [kn] | ~ 34       | ~ 10          | ~ 8    |

#### IV. FIELD EXPERIMENTS

Experiments using the SB-MPC and the IPDA-based radar tracking system were performed in the Trondheimsfjord in order to evaluate the performance in both long-range and close-quarter scenarios. The test setup and results are presented and discussed in this section.

##### A. Test setup

The ASV used is called Telemetron, which is a Polar Circle 845 Sport vessel owned by Maritime Robotics. Telemetron is a stable and highly maneuverable Rigid Buoyancy Boat (RBB). The obstacle vessels are the Trondheim Port Authority’s Munkholmen II tugboat and Kongsberg’s Ocean Space Drone I. An overview of relevant vessel specifications are provided in Table I. The vessels were equipped with the Automatic Identification System (AIS), which transmitted their position, course, and speed information. However, the AIS data was not always accurate in our tests, possibly due to significant AIS signal delays, especially when the obstacles were maneuvering. Therefore, we do not consider the AIS measurements as ground truth in our discussions.

The ASV Telemetron is equipped with the Kongsberg Seapath 330+ navigation system, which has an accuracy of  $0.1^\circ$  RMS in roll/pitch/yaw estimates, and 0.1 m RMS accuracy in position estimates. This makes accurate navigation, guidance, and control of Telemetron possible. Using the existing mission/path planning, Line-Of-Sight (LOS) guidance, and low-level vessel control software installed on Telemetron (cf. Fig. 1), we are able to achieve desired high-performance motion control according to our assumptions in Section III-C. A C++ implementation of the SB-MPC collision avoidance method was installed as part of the on-board control system (OBS), which runs on an embedded computer in the Telemetron vessel. For obstacle tracking, we use the Simrad Broadband 4G<sup>TM</sup> Radar, the Seapath 330+ navigation system, and the real-time Global Navigation Satellite System (GNSS) corrections for positioning (known as CPOS) from the Norwegian mapping authority (Kartver-

TABLE II: Radar tracking system parameters

|  |              |                                 |
|--|--------------|---------------------------------|
| Sampling time                          | $(T_r)$      | 2.8 s                           |
| Process noise covariance parameter     | $(q)$        | $(0.05 \text{ m s}^{-2})^2 I_2$ |
| Measurement noise covariance (range)   | $(R_r)$      | $(20\text{m})^2$                |
| Measurement noise covariance (bearing) | $(R_\theta)$ | $(2.3^\circ)^2$                 |
| Confirmation probability threshold     | $(P_C)$      | 0.95                            |
| Termination probability threshold      | $(P_T)$      | 0.1                             |

TABLE III: COLREGs-compliant decision parameters

|                             |                      |         |
|-----------------------------|----------------------|---------|
| Sampling time               | $(T_s)$              | 5 s     |
| Prediction horizon          | $(T)$                | 300 s   |
| Obstacle considered close   | $(d_{\text{close}})$ | 1000 m  |
| Safety distance to obstacle | $(d_{\text{safe}})$  | 185.2 m |
| Action initialization range | $(d_{\text{init}})$  | 1852 m  |

ket) [19]. The IPDA tracking algorithm is implemented in the Robot Operating System (ROS) installed on a separate computer, which has an Intel® i7 3.4 GHz CPU, running Ubuntu 16.04 Linux.

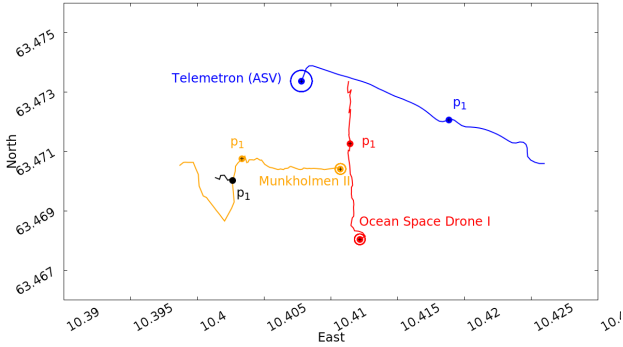
The main parameters used for both radar tracking and COLREGs-compliant decisions are shown in Table II and III, respectively. The SB-MPC method is tuned to prioritize changes in course over speed in order to produce ASV behaviors that are clear to observing operators/vessels.

##### B. Scenarios and Results

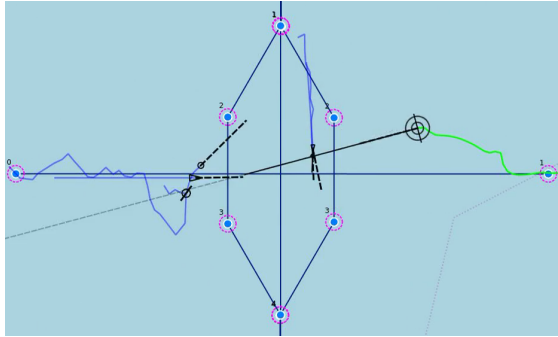
The scenarios cover both cooperating and non-cooperating obstacle situations, where the ASV is required to be proactive, but is allowed to choose reactive actions if necessary. We consider collision avoidance decisions that are made 1 nautical mile (NM) away from the target as long-range decisions, which must be COLREGs-compliant. We focus on the case where no communication exists between the ASV and the obstacles, meaning that the ASV uses only the IPDA radar tracking system installed for its collision avoidance decisions. Results from different scenarios are shown in figures 3–5.

In Fig. 3, a combined crossing and head-on situation is shown, where Fig. 3a shows the trajectories of the vessels involved, using the position estimates from the radar tracking system. The Ocean Space Drone I is well tracked from North to South, while the track of Munkholmen II is highly uncertain in the beginning. Both false tracks and track loss were experienced in this test run, with two ‘competing’ tracks (the long yellow track and the short black track) appearing for the same Munkholmen II vessel. For the COLREGs-compliant decision system, the radar tracks of Munkholmen II describe the motion of two different obstacles, and the COLREGs-compliant strategy must be robust to the uncertain motion of the obstacles.

We will use the snapshot of the vehicle control station (VCS) in Fig. 3b to discuss our observations. The VCS figure shows the planned waypoints and paths used throughout the experiments. Note that Ocean Space Drone I deviates



(a) Trajectories showing the ASV's measured position and position estimates from the radar tracking system. The end of a trajectory is indicated by the symbol  $\odot$  for the ASV and  $\ominus$  for the obstacle vessels. The position of each obstacle is enclosed by a relatively large circular safety region (cf.  $d_{\text{safe}}$  in Table III).



(b) Vehicle control station (VCS) snapshot at position  $p_1$  in Fig. 3a, showing planned waypoints, paths, and vessel trajectories obtained from both radar tracking ( $\odot$ ) and AIS values ( $\triangleright$ ).

Fig. 3: Obstacle vessels Head-on and crossing from starboard.

significantly from its planned path from North to South. This is due to the waves and eastward currents experienced during the experiments. For Munkholmen II, it is easy to compare the radar tracks (cf. Fig. 3a) with the AIS track, which is a straight line in the West-East direction. The course and track status at  $p_1$  are also shown in the VCS figure, where the symbol  $\oslash$  indicates that the short track is terminated at  $p_1$ . Before the short track was terminated it represented a significant hazard on the ASV's path, while the long track made a large deviation from the path. However, the large deviations did not lead to large reactive maneuvers by the ASV. The most critical event occurs at position  $p_1$  when the short track is terminated. The long (surviving) track has an estimated course which suggests that Munkholmen II is crossing the path of the ASV. This drastic change in situation means a significant change in collision hazard, but this leads to only a slight reaction in the ASV's behavior due to the robustness considerations in the SB-MPC strategy.

The next scenario shown in Fig. 4 describes a situation with two obstacles that do not cooperate according to COLREGs. Munkholmen II was traveling with an average speed of 6 kn ( $\sim 3$  m/s), while the Ocean Space drone's speed was about 5 kn ( $\sim 2.5$  m/s). The reference speed (10 kn) of the

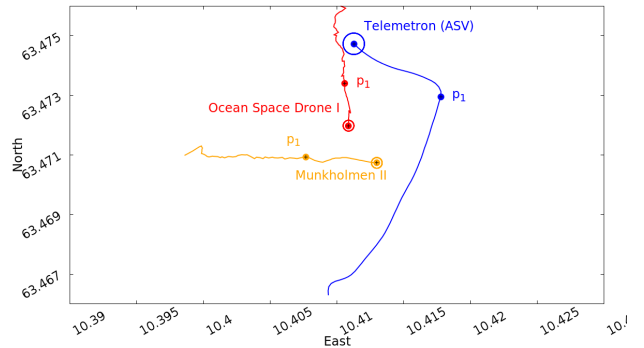


Fig. 4: Non-cooperating obstacles head-on and crossing from port. The end of a trajectory is indicated by the symbol  $\odot$  for the ASV and  $\ominus$  for the obstacles. The position of each obstacle is enclosed by a relatively large circular safety region (cf.  $d_{\text{safe}}$  in Table III).

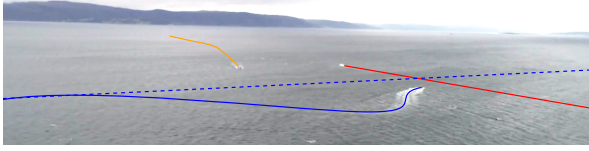
ASV allows it to make an early and clear starboard maneuver, which is adapted into a nearly straight path. The ASV's path is predictable according to COLREGs, and the ASV stays well clear of both obstacles, before heading towards its original path from position  $p_1$ . Note that both obstacles are well tracked by the IPDA tracking method, and the noise in the radar tracks does not have any significant effect on the behavior of the ASV.

We take a closer look at the course and speed estimates from the radar tracking method in the experimental results shown in Fig. 5. In Fig. 5, we test a situation where the ASV's path (from West to East) crosses the paths of both Munkholmen II and Ocean Space Drone I. An aerial photo taken during this test run is shown in Fig. 5a. Munkholmen II travels towards South, and after a while, it makes a starboard maneuver with the intention of taking partial responsibility in the head-on and crossing situation. Ocean Space Drone I on the other hand chooses a passive strategy by maintaining its course and speed. The ASV's challenging task is to understand the intentions of both obstacles based on their uncertain state estimates. The scenario is such that a wrong reaction of the ASV to Munkholmen II's starboard maneuver could easily lead to a close-quarter collision situation when Munkholmen II returns to its original (intended) course.

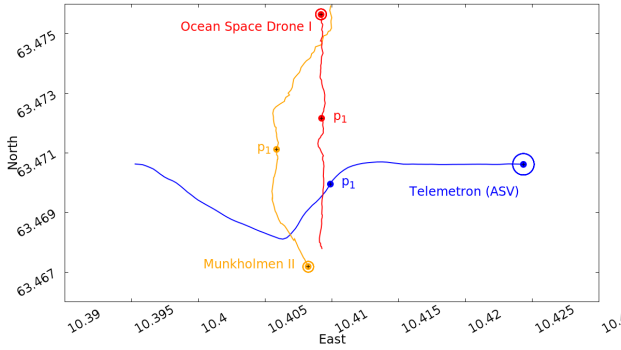
In Fig. 5c–5d, significant variations can be seen in the ASV's own course and speed measurements (partly due to the effect of waves) and estimates from the radar tracking system. The control modifications by the SB-MPC strategy show that the observed behavior of the ASV is not due to the noise in the estimates, but mainly the result of the changes in the actual collision situation and the corresponding assessment of collision hazard in the SB-MPC (cf. Section III-B).

## V. CONCLUSIONS

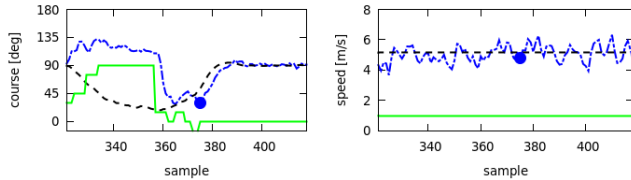
An autonomous collision avoidance system that uses an IPDA radar tracking method and SB-MPC was presented in this paper. The discussions focused on the robustness considerations made when using the SB-MPC and IPDA methods, and in particular, the case where no uncertainty estimates of obstacle tracks are obtained from the IPDA



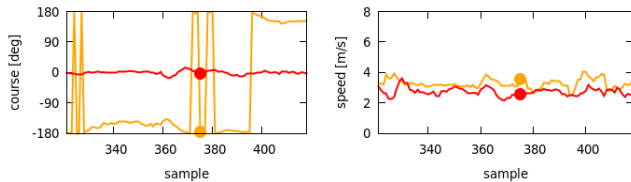
(a) Crossing situation, showing the planned (---) and actual (—) paths of the ASV, and the actual paths of Munkholmen II (—) and Ocean Space Drone I (—).



(b) Trajectories showing the ASV's measured position and position estimates from the radar tracking system. The end of a trajectory is indicated by the symbol  $\odot$  for the ASV and  $\ominus$  for the obstacle vessels. The position of each obstacle is enclosed by a relatively large circular safety region (cf.  $d_{\text{safe}}$  in Table III).



(c) Desired value from LOS guidance (---), SB-MPC modification (—), and measured value (---). Compare SB-MPC modifications with desired values from LOS guidance. The points represent  $p_1$  in Fig. 5b.



(d) Obstacle course and speed values from IPDA radar tracking. The colors correspond to the trajectories in Fig. 5b, and the points represent  $p_1$ .

Fig. 5: Obstacle vessels crossing from both port and starboard.

tracking method for making collision avoidance decisions. Results from full-scale experiments were discussed, and the results show that the IPDA radar tracking method produces obstacle track estimates suitable for collision avoidance, and the SB-MPC method is capable of handling uncertain tracks in its decision process in both close-quarter and long-range scenarios.

## ACKNOWLEDGMENT

We would like to thank Maritime Robotics for making Telemetron available for our experiments, and Kongsberg Maritime for providing their navigation system. We are

grateful to Stephanie Kemna and Arild Hepsø from Maritime Robotics for helping with everything concerning Telemetron. We also thank Knut Gunnar Knutsen, the captain of the Munkholmen II vessel, and Rune Simonsen, the operator of the Ocean Space Drone I, for their cooperation.

## REFERENCES

- [1] IMO, "Convention on the International Regulations for Preventing Collisions at Sea, (COLREGs)," 1972. [Online]. Available: <http://www.imo.org/en/About/conventions/listofconventions/pages/colreg.aspx>
- [2] E. F. Wilthil, A. L. Flåten, and E. F. Brekke, "A target tracking system for ASV collision avoidance based on the PDAF," in *Sensing and Control for Autonomous Vehicles: Applications to Land, Water and Air Vehicles*, T. I. Fossen, K. Y. Pettersen, and H. Nijmeijer, Eds. Springer International Publishing, 2017, pp. 269–288.
- [3] D. Hermann, R. Galeazzi, J. Andersen, and M. Blanke, "Smart Sensor Based Obstacle Detection for High-Speed Unmanned Surface Vehicle," *IFAC-PapersOnLine*, vol. 48, no. 16, pp. 190 – 197, 2015.
- [4] L. Elkins, D. Sellers, and W. R. Monach, "The autonomous maritime navigation (amn) project: Field tests, autonomous and cooperative behaviors, data fusion, sensors, and vehicles," *Journal of Field Robotics*, vol. 27, no. 6, pp. 790–818.
- [5] M. Schuster, M. Blaich, and J. Reuter, "Collision Avoidance for Vessels using a Low-Cost Radar Sensor," *IFAC Proceedings Volumes*, vol. 47, no. 3, pp. 9673 – 9678, 2014, 19th IFAC World Congress.
- [6] B. H. Eriksen, E. F. Wilthil, A. L. Flåten, E. F. Brekke, and M. Breivik, "Radar-based maritime collision avoidance using dynamic window," in *2018 IEEE Aerospace Conference*, March 2018, pp. 1–9.
- [7] D. K. M. Kufoalor, E. F. Brekke, and T. A. Johansen, "Proactive Collision Avoidance for ASVs using A Dynamic Reciprocal Velocity Obstacles Method," in *Proceedings of the 2018 IEEE/RSJ International Conference on Intelligent Robots and Systems (IROS)*, Madrid, Spain, 2018.
- [8] T. A. Johansen, T. Perez, and A. Cristofaro, "Ship Collision Avoidance and COLREGS Compliance Using Simulation-Based Control Behavior Selection With Predictive Hazard Assessment," *IEEE Transactions on Intelligent Transportation Systems*, vol. 17, no. 12, pp. 3407–3422, Dec 2016.
- [9] Y. Kuwata, M. T. Wolf, D. Zanzhitzky, and T. L. Huntsberger, "Safe Maritime Autonomous Navigation With COLREGS, Using Velocity Obstacles," *IEEE Journal of Oceanic Engineering*, vol. 39, no. 1, pp. 110–119, Jan 2014.
- [10] P. Svec, B. C. Shah, I. R. Bertaska, J. Alvarez, A. J. Sinisterra, K. von Ellenrieder, M. Dhanak, and S. K. Gupta, "Dynamics-aware target following for an autonomous surface vehicle operating under COLREGS in civilian traffic," in *2013 IEEE/RSJ International Conference on Intelligent Robots and Systems*, 2013, pp. 3871–3878.
- [11] M. R. Benjamin, J. J. Leonard, J. A. Curcio, and P. Newman, "A method for protocol-based collision avoidance between autonomous marine surface craft," *J. Field Robotics*, vol. 23, pp. 333–346, 2006.
- [12] C. Tam, R. Bucknall, and A. Greig, "Review of Collision Avoidance and Path Planning Methods for Ships in Close Range Encounters," *Journal of Navigation*, vol. 62, no. 3, p. 455476, 2009.
- [13] T. Statheros, G. Howells, and K. M. Maier, "Autonomous Ship Collision Avoidance Navigation Concepts, Technologies and Techniques," *Journal of Navigation*, vol. 61, no. 1, p. 129142, 2008.
- [14] I. B. Hagen, D. K. M. Kufoalor, E. F. Brekke, and T. A. Johansen, "MPC-based Collision Avoidance Strategy for Existing Marine Vessel Guidance Systems," in *Proceedings of the 2018 IEEE International Conference on Robotics and Automation*, Brisbane, Australia, 2018.
- [15] X. R. Li and V. P. Jilkov, "Survey of maneuvering target tracking. Part I. Dynamic models," *IEEE Transactions on Aerospace and Electronic Systems*, vol. 39, no. 4, pp. 1333–1364, Oct 2003.
- [16] E. F. Wilthil, E. Brekke, and O. B. Asplin, "Track initiation for maritime radar tracking with and without prior information," in *21st International Conference on Information Fusion*, 2018, pp. 1–8.
- [17] D. Mušicki, R. Evans, and S. Stankovic, "Integrated probabilistic data association," *IEEE Transactions on Automatic Control*, vol. 39, no. 6, pp. 1237–1241, Jun 1994.
- [18] Y. Bar-Shalom and X.-R. Li, *Multitarget-Multisensor Tracking: Principles and Techniques*. YBS Publishing, 1995.
- [19] Kartverket, "Positioning (CPOS)," Sep. 2018. [Online]. Available: <https://kartverket.no/en/Positioning/>